

Biologically Plausible Training Mechanisms for Self-Supervised Learning in Deep Networks

Mufeng Tang, Yibo Yang, Yali Amit

July 25, 2022

Abstract

We develop biologically plausible training mechanisms for self-supervised learning (SSL) in deep networks. SSL, with a contrastive loss, is more natural as it does not require labelled data and its robustness to perturbations yields more adaptable embeddings. Moreover the perturbation of data required to create positive pairs for SSL is easily produced in a natural environment by observing objects in motion and with variable lighting over time. We propose a contrastive hinge based loss whose error involves simple local computations as opposed to the standard contrastive losses employed in the literature, which do not lend themselves easily to implementation in a network architecture due to complex computations involving ratios and inner products. Furthermore we show that learning can be performed with one of two more plausible alternatives to backpropagation. The first is difference target propagation (DTP), which trains network parameters using target-based local losses and employs a Hebbian learning rule, thus overcoming the biologically implausible symmetric weight problem in backpropagation. The second is simply layer-wise learning, where each layer is directly connected to a layer computing the loss error. The layers are either updated sequentially in a greedy fashion (GLL) or in random order (RLL), and each training stage involves a single hidden layer network. The one step backpropagation needed for each such network can either be altered with fixed random feedback weights as proposed in [1], or using updated random feedback as in [2]. Both methods represent alternatives to the symmetric weight issue of backpropagation. By training convolutional neural networks (CNNs) with SSL and DTP, GLL or RLL, we find that our proposed framework achieves comparable performance to its implausible counterparts in both linear evaluation and transfer learning tasks.

1 Introduction

The rapid development of deep learning in recent years has raised extensive interest in applying artificial neural networks (ANNs) to the modelling of cortical computations. Multiple lines of research, including those using convolutional neural networks (CNNs) to model processing in the ventral visual stream [3, 4], and those using recurrent neural networks (RNNs) as models of generic cortical computation [5, 6], have suggested that ANNs are not only able to replicate behavioral activities (e.g. categorization) of biological systems, but also capable of reproducing unit-level activities observed in vivo or in vitro. These observations, combined with the structural similarities (e.g. a hierarchy of layers and recurrent connections) between ANNs and cortical areas, make the use of deep learning a promising approach to the modelling of neural computations.

Despite these successes, there are some fundamental problems confronting this approach. One issue with classification ANNs as a model for cortical learning is their reliance on massive amounts of labelled data, another limitation is the lack of invariance to perturbations not observed in the training data, finally most ANN’s employ backpropagation for learning. To be more specific, modern classification ANNs are trained to match their predictions to a set of target labels each associated with a training data point (e.g. an image), while biological systems, such as humans, usually learn without a large degree of supervision. In addition, ANNs trained in this way cannot generalize well to other datasets than the ones they are trained on, i.e. they are less capable of transfer learning. In contrast, biological systems are very robust to the change of tasks and can generalize knowledge learned on one task to another pretty well. Finally, backpropagation (BP), the learning rule for modern ANNs employing the chain rule for differentiation [7], is biologically implausible, as the same set of synaptic weights that have been used to compute the feedforward signals are also needed to compute the feedback error signals. Such a symmetric synaptic weight matrix does not exist in the brain [2, 8, 9].

In recent years, a number of solutions have been proposed to address the learning rule issue [10, 8, 2, 11]. However, to our knowledge, none have considered the learning rule problem together with the issue of robustness to variation and the need for massive labeled data sets. To tackle these issues, we draw inspiration from the self-supervised learning (SSL) methods [12, 13], which have been popular in recent years in deep learning but in fact have a rather long history [14]. Rather than relying on labels as external teaching signals, SSL methods train neural networks with an objective function that attempts to maximize the agreement between two separate but related views of an input, each serving as the internal teaching signal for the other. In computer vision, these two views are usually created by different data augmentation techniques, such as random crop and color jittering. Since such an objective alone would cause the networks to produce a constant embedding regardless of the inputs (collapsing), different SSL methods employ different regularization terms to prevent collapsing, typically using negative examples: images that are unrelated to the pair of related views. Note that the motion of a 3d object provides the jittering effect in a natural environment, including changes in lighting. The brain would then record a pair of images of the moving object and keep a few ‘negative’ unrelated images in memory, to update the network.

The ultimate outcome is an embedding of the data with strong representation and invariance properties. Using SSL as a network pre-training technique, multiple lines of research have shown that they can produce embeddings comparable to those from networks trained by supervised methods in downstream tasks such as linear evaluation, namely training a linear classifier on labelled data using the learned embedding. They also perform well in transfer learning [12, 13]. We are interested in SSL not only because of its independence of labelled data, but also due to its invariance to perturbations in testing data, which make it a particularly suitable computational model for learning in cortical areas. In this work, we also propose several ways to implement the SSL methods using more biologically plausible learning rules that have been proposed for labelled data.

One biologically plausible learning rule mentioned above is difference target propagation (DTP) [10]. Rather than backpropagating the global loss top-down using the chain rule, DTP updates the weights in a network by minimizing a set of local losses, computed as the difference between the bottom-up forward activities and the top-down targets, which are propagated through a set of non-linear functions. The localized losses in DTP then yield a Hebbian learning rule for the connectivity weights. For computer vision tasks with DTP, previous works [15] suggested that pooling layers in CNNs are not compatible with this learning rule, and used strided convolutional layers to perform down-sampling of input data. We nevertheless find that pooling layers can in fact be incorporated into networks trained by DTP, increasing the flexibility of this algorithm in various network architectures.

Another approach we explore is layer-wise learning, where each layer has a direct connection to the layer computing the self-supervised loss, and updates a single hidden layer with input given by the output of the previous layer. Such learning can be done sequentially bottom up, or randomly, updating a different random layer for each batch. The sequential form of learning has been studied in a number of papers [16, 17, 18, 19, 20, 21]. However the sequential approach requires rigid timing of the updates of each layer, which would seem unlikely in the biological setting. Randomizing the layers being updated at each step seems more plausible as a biological mechanism. We believe such random layer-wise learning is a novel contribution of this paper.

All previous approaches to layer-wise learning train the current updated hidden layer using backpropagation, which still assumes symmetric connectivity between the output layer and the hidden layer. We also explore the possibility of using the random feedback (RF) approach of [1], which uses a fixed set of random feedback weights connecting the output layer to the hidden layer, to overcome the symmetry problem described above. This method works well with shallow networks (in this case one hidden layer) but its performance deteriorates with the depth of the network. It is thus quite suitable for layer-wise learning. An alternative, updated random feedback (URF), proposed in [2], is to use the same updates to the forward and backward connections starting at random initial conditions as opposed to imposing strict symmetry. This approach works nearly as well as backpropagation and yields identical results on shallow networks.

We experiment with the SIMCLR method proposed in [22] but we replace the original self-supervised loss with a more biologically plausible loss. The original SIMCLR loss requires the normalization of the embeddings to unit length, a complex operation involving interactions between all units of the output layer. Furthermore it involves a ratio between outputs of

different examples in the batch. Our loss, called the contrastive hinge loss and which is motivated by a similar proposal in [2] avoids normalization and uses a simple comparison of thresholded outputs. We emphasize that the aim of our work is not to achieve state-of-the-art performances on the datasets we use, but rather, we focus on the comparison between our framework and those with implausible features such as backpropagation, the SIMCLR loss, and deep supervised learning.

This paper is organized as follows. In section 2 we discuss related works in SSL learning and in biologically plausible learning rules. In section 3 we describe the technical details of SSL, DTP, and layer-wise learning, as well as the proposed loss that contributes to the biological plausibility and flexibility of this framework. In section 4 we present the experimental results, including our proposed framework’s performance in linear evaluation and transfer learning tasks. We conclude with a discussion section.

2 Related Work

Biologically Plausible Learning Rules. The biological implausibility of backprop was mentioned in [9] and they first suggested to separate the feedforward weights of ANNs from the feedback weights. More recently, [1] proposed a biologically plausible learning rule called “feedback alignment” (FA), which decouples the feedforward and feedback weights by fixing the feedback weights at random values, we rename this “random feedback” (RF). However, this method does not scale well to deeper networks and more challenging datasets [2]. Several modifications have been proposed to improve the performance of FA. [23] found that using Batch Normalization (BN) could improve the performance of FA, but it is unclear how BN can be employed by biological neural circuits.

Another track of research on the improvement of FA focuses on finding a learning rule for the feedback weights (rather than fixing them). [2] proposed to train the randomly initialized feedback weights using the same updates as those for the feedforward weights, and found a significant improvement of error rates in deeper networks, hence the name “updated random feedback” (URF). This work also paid particular attention to the topmost layer. By modifying the loss for supervised learning, the learning rule at the topmost in this method yields a Hebbian update and is thus more biologically plausible than the softmax loss. In our work we follow this idea and propose a more biologically plausible loss for SSL. Similar to [2], [11] also proposed a learning rule for the feedback weights that will force the feedback weights to converge to the feedforward weights, resulting in a convergence to backprop.

An alternative modification of deep learning yielding more biologically plausible update rules is DTP [10]. Localized losses are introduced in all layers, such that the weight updates are purely local and independent of the outgoing weights. The backward computation in DTP propagates the “targets” top-down and uses a set of backward weights learned through layer-wise autoencoders. This structure on the basis of layer-wise losses connects DTP to predictive coding [24, 25, 26, 27], which have formed a well-established computational model for brain areas such as visual cortex. However, these latter works on predictive coding still suffer from the symmetric weight problem, which is avoided in DTP. [15] further investigated DTP with CNNs and more challenging datasets such as CIFAR10, and found a significant

performance gap between backprop and DTP in supervised visual tasks such as classification. They also experimented with locally connected layers as a biologically more realistic surrogate for convolutional layers.

In end-to-end learning, all layers in the network, after passing the input signal forward to the next layer, must wait for the signal to feed-forward through the rest of the network and the error signal to propagate back from the last layer. No updates can be done during this period. This constraint is referred to as the locking problem by Jaderberg et al [20]. Moreover end-to-end learning requires some mechanism of passing information sequentially through multiple layers, whether using backpropagation or target propagation.

Layer-wise learning is an alternative to end-to-end learning that tackles both problems. Greedy unsupervised layer-wise learning was first proposed to improve the initialization of deep supervised neural networks [16, 17]. [18] used the layer-wise method to train residual blocks in ResNet sequentially, then refined the network with the standard end-to-end training. [19] studied the progressive separability of layer-wise trained supervised neural networks and demonstrated Greedy layer-wise Learning (GLL) can scale to large-scale datasets like ImageNet. Other attempts at supervised layer-wise learning involve a synthetic gradient [20] and a layer-wise loss that combines local classifier and similarity matching loss [21].

Self-supervised Learning. The idea of SSL was originally proposed in 1992 by [14]. The authors of this work used a self-supervised objective that maximizes the agreement between the representations of two related views of an input, subject to how much they both vary as the input is varied. However, it was not until 2020 that SSL was formally introduced to modern deep learning and applied to computer vision tasks, by [12] and [13].

Borrowing ideas from the Contrastive Predictive Coding (CPC) framework by [28], these methods introduced the concept of contrasts to prevent collapse. In these methods, the self-supervised objective includes a term that maximizes the agreement between related representations (“positives”), as well as a term to minimize the agreement between unrelated representations (“negatives”), thus preventing the networks from producing a constant output regardless of the inputs. Optimizing this objective will create contrasts between positives and negatives, hence the term *contrastive learning*. The acquisition of positives is similar across different contrastive methods, using random perturbations of the input. The selection of negatives is what differentiates them.

The SIMCLR framework, proposed by [12], uses all other images within a mini-batch as negatives of an image. In this way, the batch size is associated with the number of negatives and usually needs to be large enough to provide sufficient negatives. To decouple these two hyperparameters, the MoCo framework, by [13], uses a dynamic queue of negatives, with its length decoupled from the batch size. During training, every new mini-batch is enqueued and the oldest mini-batch is dequeued, which provides a larger sample of negatives from the continuous space of images.

More recently, a few new methods in self-supervised learning have been proposed to eliminate the need for negatives (therefore no contrast), including BYOL [29], SIMSIAM [22] and Barlow Twins [30]. BYOL and SIMSIAM both used a top-layer linear predictor and a gradient blocker to asymmetrize the two networks for the pair of positives, and the performance of their idea proved to be comparable to the contrastive methods. However,

currently there is a lack of theoretical support for this track of negative-free SSL methods, as in why the asymmetric structure prevents collapsing. Barlow Twins uses a symmetric architecture, and their objective function enforces the cross-correlation matrix between the positives to be as close to an identity matrix as possible. Compared to the two other negative-free SSL methods, it is easier to see why Barlow Twins stops collapsing, and its objective also has a biological interpretation closely related to the redundancy reduction principle [31], which has been used to describe how the cortical areas process sensory inputs. We do not experiment with Barlow Twins in this paper, as we are still exploring biologically plausible ways to implement this loss.

None of the studies mentioned above have focused on the biological plausibility of SSL. To our knowledge, [32] is the only study so far that used SSL as a model for biological learning. Using the techniques developed by [3] and [33], they measured the correlation between recordings of neuronal activities from the ventral visual stream and unit activities of CNNs trained by SIMCLR, given the same visual inputs and tasks. The CNNs were found to achieve highly accurate neuronal activity predictions in multiple ventral visual cortical areas, even more so than CNNs trained with supervised learning. However, the CNN models in their experiments are trained with backprop, and we argue that it is hard to conceive of the original objective function of SIMCLR being computed using neural circuits. We suggest an alternative simpler loss that could be implemented with simple neural circuits.

3 Methods

In this section we first describe the symmetric weight problem in BP. Then we introduce both DTP and RF, and describe how they resolve the symmetric weight problem. Considering that both algorithms have suffered from performance degradation under certain circumstances (i.e. DTP with CNNs and RF with deeper networks), we propose modifications to remedy these problems. Finally we describe the SSL framework, particularly in terms of its biological plausibility.

3.1 Weight Symmetry in BP

We first define the notation for a multilayer network with layers $1, 2, \dots, L$. We denote the activation value of the i th neuron in l th layer as $x_{l,i}$, and the total number of neurons in this layer as n_l . We denote the feedforward weight from the j th neuron in the $(l-1)$ th layer to the i th neuron in the l th layer as $W_{l,ij}$, the forward computation in this neuron can be written as:

$$x_{l,i} = \sigma(h_{l,i}), \quad h_{l,i} = \sum_{j=1}^{n_{l-1}} W_{l,ij} x_{l-1,j} \quad (1)$$

where σ is the element-wise non-linearity. Written in matrix form, where $\mathbf{x}_l \in \mathbb{R}^{n_l}$, $\mathbf{x}_{l-1} \in \mathbb{R}^{n_{l-1}}$ and $\mathbf{W}_l \in \mathbb{R}^{n_l \times n_{l-1}}$, this is:

$$\mathbf{x}_l = \sigma(\mathbf{h}_l), \quad \mathbf{h}_l = \mathbf{W}_l \mathbf{x}_{l-1} \quad (2)$$

In the top layer, where no non-linearity will be applied, the forward computation will be $\mathbf{x}_L = \mathbf{W}_L \mathbf{x}_{L-1}$ and a global loss $\mathcal{L}(\mathbf{x}_L, \mathbf{y})$ will be computed based on the true labels vector \mathbf{y} and final layer activities \mathbf{x}_L in supervised learning.

The difficulty in imagining a biological implementation of BP has been discussed extensively [9, 8] and boils down to the need for symmetric synaptic connections between neurons in order to propagate the error backwards through the layers. Following the feed-forward pass above, in BP the update of the weight matrix \mathbf{W}_l is computed as follows:

$$\Delta \mathbf{W}_l = \frac{\partial \mathcal{L}}{\partial \mathbf{h}_l} \mathbf{x}_{l-1}^T = \delta_l \mathbf{x}_{l-1}^T \quad (3)$$

$$\delta_l = \frac{\partial \mathcal{L}}{\partial \mathbf{x}_l} \frac{\partial \mathbf{x}_l}{\partial \mathbf{h}_l} = \sigma'(\mathbf{h}_l) \mathbf{W}_{l+1}^T \delta_{l+1} \quad (4)$$

where δ_l is referred to as the error signal, and $\sigma'(\mathbf{h}_l)$ is a diagonal matrix with the i -th diagonal element being $\sigma'(h_{l,i})$. The need for the outgoing weight \mathbf{W}_{l+1} when computing the update of the weight matrix introduces the symmetric weight problem.

3.2 Layer-wise Learning with Random Feedback

Random Feedback (RF). This tackles the symmetric weight problem by simply replacing the weight \mathbf{W}_{l+1}^T in (4) with a fixed random matrix \mathbf{B}_{l+1} , i.e. the error signal in RF is computed as:

$$\delta_l = \sigma'(\mathbf{h}_l) \mathbf{B}_{l+1} \delta_{l+1} \quad (5)$$

Although proven to be comparable to BP in shallow networks, the performance of RF degrades as network depth increases, due to the fact that the alignment between \mathbf{W}_{l+1} and \mathbf{B}_{l+1} weakens [2]. We thus combine RF with layer-wise learning, where the RF error signals (5) are always computed in a shallow, 1-layer network, to tackle this issue with depth.

Updated Random Feedback (URF). In [2] a more plausible version of BP is proposed, where the random feedback weights \mathbf{B}_l , which are initialized differently from the feedforward weights, are updated with the same increment as the feedforward weights, as defined in (3). The updated random feedback (URF) method yields results very close to BP, essentially indistinguishable for shallow networks. We compare the performance of RF with the one layer BP/URF in the context of layer-wise training.

Greedy and Randomized Layer-wise Learning. We adapted the supervised Greedy Layer-wise Learning (GLL) [19] method to self-supervised learning by training convolutional layers sequentially with auxiliary heads and self-supervised loss, as shown in Figure 1. The base encoders are trained layer by layer. For each layer, the new training layer is added on top of the previous architecture, and only parameters in the new training layer and its auxiliary head are updated. Thus at each step we are training a network with one hidden layer. Then, we replace the auxiliary heads with a linear classifier layer and only updates these weights with supervised learning to measure the representational power of the embedding. The

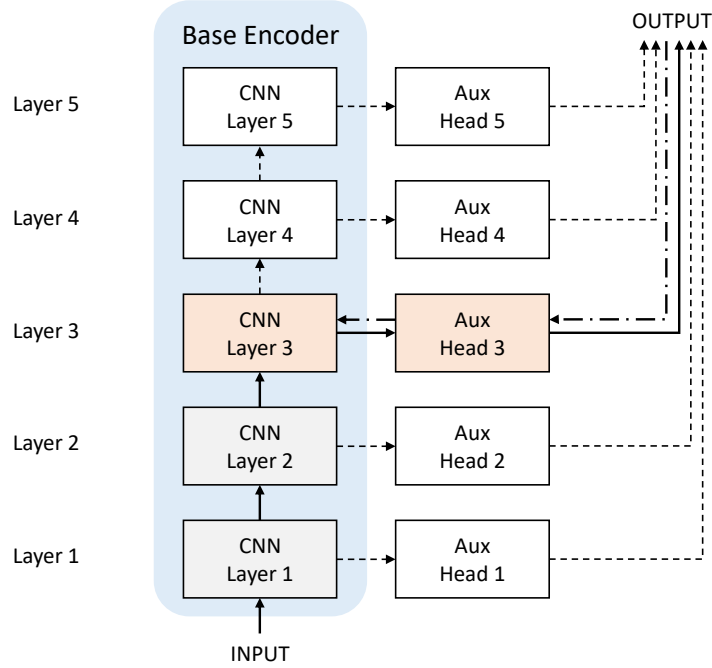


Figure 1: Diagram of the training process. When training layer 3, for example, as shown in the diagram, only the shaded blocks are included in the network, and only layer 3 of the network and the auxiliary head 3 are updated. Solid arrows indicate feed-forward paths and dash-dotted arrows indicate feedback paths. For Greedy Layer-wise Learning (GLL), CNN layers are trained till convergence sequentially from down to top. For Randomized Layer-wise Learning (RLL), a layer is randomly selected to train for each batch of training data.

pretrained network with self-supervised learning provides the encoder input to the classifier and is not updated.

GLL tackles the locking problem as it does not require back-propagating through the whole network to get the full gradients. It does not require storage of activations in intermediate layers. In addition to GLL, where we sequentially train layers with auxiliary heads, we also explore what we called Randomized Layer-wise Learning (RLL), where a random layer in the architecture is selected to update for each batch of training data. The data is first passed through the layers before the selected layer, then the selected layer and corresponding auxiliary classifier. Only parameters in the selected layer and its auxiliary head are updated. RLL maintains the main advantage of GLL in terms of plausibility, in that only one hidden layer is updated, requiring minimal error propagation, and, in addition, it does not require the sequential training of the network, which assumes strict timing of the layer updates.

3.3 Difference Target Propagation with Pooling Layers

Target propagation (TP) circumvents the symmetric weight problem using layer-local losses. The main idea behind TP is to set a *target* for each layer in the network, such that by reducing the distance between the feedforward activity and the feedback target in each layer, the global loss would be reduced as well. For the activity vector \mathbf{x}_l at the l th layer, we denote its corresponding target as $\hat{\mathbf{x}}_l$, and target propagation aims to minimize a layer local loss:

$$\mathcal{L}_l = \frac{1}{2} \|\mathbf{x}_l - \hat{\mathbf{x}}_l\|_2^2 \quad (6)$$

The error signal is thus purely based on the local losses:

$$\delta_l = \frac{\partial \mathcal{L}_l}{\partial \mathbf{x}_l} \frac{\partial \mathbf{x}_l}{\partial \mathbf{h}_l} = (\mathbf{x}_l - \hat{\mathbf{x}}_l) \sigma'(\mathbf{h}_l) \quad (7)$$

As can be seen, the dependence of the weight gradient on the outgoing feedforward weights is eliminated by this layer-local loss. The remaining question is how to find the targets corresponding to the forward activities.

The ultimate goal of both TP and BP is to reduce a global loss \mathcal{L} . BP achieves this directly by using the chain rule, while for TP, this is achieved by choosing targets such that the minimization of the layer-local losses \mathcal{L}_l (i.e. pulling \mathbf{x} closer to $\hat{\mathbf{x}}$) also minimizes the global loss \mathcal{L} . Specifically, we would like to satisfy the global condition:

$$\mathcal{L}(\mathbf{x}_L(\hat{\mathbf{x}}_l, \mathbf{W}^{L,l}), \mathbf{y}) < \mathcal{L}(\mathbf{x}_L(\mathbf{x}_l, \mathbf{W}^{L,l}), \mathbf{y}) \quad (8)$$

We use the notation $\mathbf{x}_L(\mathbf{x}_l, \mathbf{W}^{L,l})$ to emphasize the impact of the target in the l th layer on the global loss, where $\mathbf{W}^{L,l}$ is the set of all weight matrices between the l th layer and the top layer. This global condition can be reduced to local conditions at each layer l :

$$\mathcal{L}_l(f_l(\hat{\mathbf{x}}_{l-1}), \hat{\mathbf{x}}_l) < \mathcal{L}_l(f_l(\mathbf{x}_{l-1}), \hat{\mathbf{x}}_l) \quad (9)$$

where $f_l(\mathbf{x}_{l-1}) = \sigma(\mathbf{W}_l \mathbf{x}_{l-1})$. In other words, if the distance between the forward activity and target at the $(l-1)$ th layer is small enough ($\mathbf{x}_{l-1} \rightarrow \hat{\mathbf{x}}_{l-1}$), the distance between the target and forward activity at the l th layer will also be reduced. The smaller distance between the target and forward activity in the l th layer will yield the reduction of the distance in the $(l+1)$ th layer if this condition is satisfied there as well, and thus at the topmost layer we have:

$$\mathcal{L}_L(f_L(\hat{\mathbf{x}}_L), \hat{\mathbf{x}}_{L+1}) < \mathcal{L}_L(f_L(\mathbf{x}_L), \hat{\mathbf{x}}_{L+1}) \quad (10)$$

For supervised learning, $f_L(\mathbf{x}_L) = \mathbf{W}_L \mathbf{x}_L$, and if we set the target $\hat{\mathbf{x}}_{L+1} = \mathbf{y}$, and $\mathcal{L}_L = \mathcal{L}$ to be the softmax cross-entropy loss (or any other loss for supervised learning), minimizing the loss in the topmost layer will improve the classification performance. The layer-local optimizations thus produce a global optimization.

In order to find this set of layer-local targets able to “forward propagate” the optimizations of local objectives to the optimization of the global objective, TP first set the topmost target using gradient descent directly from the global objective:

$$\hat{\mathbf{x}}_L = \mathbf{x}_L - \eta_L \frac{\partial \mathcal{L}}{\partial \mathbf{x}_L} \quad (11)$$

so that minimizing $\|\mathbf{x}_L - \hat{\mathbf{x}}_L\|_2^2$ definitely minimizes the global objective. We then compute the intermediate-layer targets using a backward non-linear function g_l such that:

$$\hat{\mathbf{x}}_{l-1} = g_l(\hat{\mathbf{x}}_l), \quad l = L-1, \dots, 2 \quad (12)$$

where $g_l(\hat{\mathbf{x}}_l) = \sigma(\mathbf{V}_l \hat{\mathbf{x}}_l)$ and $\mathbf{V}_l \in \mathbb{R}^{n_{l-1} \times n_l}$ is a trainable parameter. Notice that, if the corresponding forward function f_l is invertible and g_l is exactly f_l^{-1} , we have:

$$\hat{\mathbf{x}}_{l-1} = f_l^{-1}(\hat{\mathbf{x}}_l) \quad (13)$$

$$\mathcal{L}_l(\hat{\mathbf{x}}_l, f_l(\hat{\mathbf{x}}_{l-1})) = \mathcal{L}_l(\hat{\mathbf{x}}_l, f_l(f_l^{-1}(\hat{\mathbf{x}}_l))) = \mathcal{L}_l(\hat{\mathbf{x}}_l, \hat{\mathbf{x}}_l) < \mathcal{L}_l(\hat{\mathbf{x}}_l, f_l(\mathbf{x}_{l-1})) \quad (14)$$

In other words, if the backward function g_l is exactly the inverse of f_l , the condition in equation (9) will definitely be satisfied. Since an exact inverse usually does not exist in a feedforward neural network, where the embedding size decreases as the network deepens, it is therefore a natural choice to train g_l to be an approximate inverse of f_l at $\hat{\mathbf{x}}_l$. These inverses can be obtained by training a set of layer-wise autoencoders with the following local loss:

$$\mathcal{L}_l^{inv} = \|g_l(f_l(\mathbf{x}_{l-1})) - (\mathbf{x}_{l-1})\|_2^2 \quad (15)$$

The algorithm described above is vanilla target propagation, while Difference Target Propagation (DTP) is inspired by the ‘‘stabilization problem’’ [10]. In TP, as the target of the lower layers are determined by their adjacent upper layers, when the local loss in the upper layer is minimized, i.e. $\hat{\mathbf{x}}_l = \mathbf{x}_l$, it is also desirable that in the lower layer $\hat{\mathbf{x}}_{l-1} = \mathbf{x}_{l-1}$, so that the update of the activation in the lower layer will stop and thus will not change the value of the upper layer and break the equilibrium there. However, vanilla TP does not have this property. To address this issue, [10] proposed the ‘‘difference target propagation’’ (DTP), where the target is computed as follows:

$$\hat{\mathbf{x}}_{l-1} = \mathbf{x}_{l-1} + g_l(\hat{\mathbf{x}}_l) - g_l(\mathbf{x}_l) \quad (16)$$

In this way, once the equality holds between the target and the forward activity in the l th layer, the same equality holds for the $(l-1)$ th layer as well. A proof showing that the targets computed in this way will also satisfy the local condition specified in equation (9) can be found in [10]. The full algorithm for DTP is shown in Algorithm 1.

Incorporating Pooling Layers into DTP. So far we have only discussed DTP in simple multi-layer perceptrons (MLPs). In CNNs, the forward functions f_l and backward functions g_l have more complex structures. Convolutional layers are interleaved with pooling layers to perform down-sampling of the data, and thus f_l is modelled as the combination of a convolutional layer and the subsequent pooling layers. [15] claimed that pooling layers, which contain a deterministic step (either averaging or taking maximum), is incompatible

Algorithm 1 Difference Target Propagation

1: Initialization:	13: end for
2: forward functions $f_l, l = 1, \dots, L$	14:
3: backward functions $g_l, l = 1, \dots, L - 1$	15: Set the first target: $\hat{\mathbf{x}}_L = \mathbf{x}_L - \eta_L \frac{\partial \mathcal{L}_L}{\partial \mathbf{x}_L}$
4: input \mathbf{x}_0	16: for $l = L$ to 2 do
5:	17: $\hat{\mathbf{x}}_{l-1} = \mathbf{x}_{l-1} - g_l(\mathbf{x}_l) + g_l(\hat{\mathbf{x}}_l)$
6: for $l = 1$ to L do	18: end for
7: $\mathbf{x}_l = f_l(\mathbf{x}_{l-1})$	19:
8: end for	20: for $l = 1$ to L do
9:	21: $\mathcal{L}_l = \ f_l(\mathbf{x}_{l-1}) - \hat{\mathbf{x}}_l\ _2^2$ if $l < L$
10: for $l = L$ to 2 do	22: $\mathcal{L}_l = \mathcal{L}$ if $l = L$
11: $\mathcal{L}_l^{inv} = \ g_l(f_l(\mathbf{x}_{l-1})) - \mathbf{x}_{l-1}\ _2^2$	23: Update parameters in f_l by minimizing \mathcal{L}_l
12: Update parameters in g_l by minimizing \mathcal{L}_l^{inv} using SGD	using SGD
	24: end for

with DTP, as the inverse of this deterministic step can hardly be modelled using a simple nonlinear function g_l . Instead, they used strided convolutional layers to model f_l and strided deconvolutional layers to model g_l to perform down-sampling and the inverse up-sampling. However, we observe that we can retain pooling layers in the forward pass, i.e. $f_l = \text{CONV} + \text{POOLING}$, but use strided deconvolutional layers in the backward pass to approximate the inverse of the forward function, i.e. $g_l = \text{STRIDED DECONV}$. Essentially, this arrangement will enforce the strided deconvolution to learn the unpooling operation. A comparison of the results in the Experiments section below demonstrates that incorporating max-pooling significantly improves the linear evaluation performances.

3.4 Self-supervised learning

The fundamental assumption of self-supervised learning (SSL) is that if a network is trained to maximize the agreement between two separate but related views of an input (e.g. an image of an object) it can learn to embed different views of the object close by in an embedding space. The hope is that this type of invariance will translate to successful linear classification using the embedding as input. The two views of the object serve as internal teaching signals for each other that are unsupervised. This eliminates the need for multi-layer learning with labelled data. Moreover it allows the network to learn the invariant embedding with data from images with unknown classes, possibly disjoint from the classes for which classification is ultimately required.

Merely maximizing the agreement between views causes the networks to produce a constant embedding regardless of the inputs (“collapsing”), and thus different SSL methods focus on different constraints to this agreement maximization objective to prevent collapsing. Most SSL methods used in computer vision create the related views through a data augmentation (distortion) step \mathcal{T} (Figure 2), which includes random crop, flip, rotation and color jittering. Given a batch of images, for each image \mathbf{x}_0 we create a randomly distorted view called \mathbf{x}_0^p . Both \mathbf{x}_0 and \mathbf{x}_0^p are then passed into the same base encoder network $f(\cdot)$

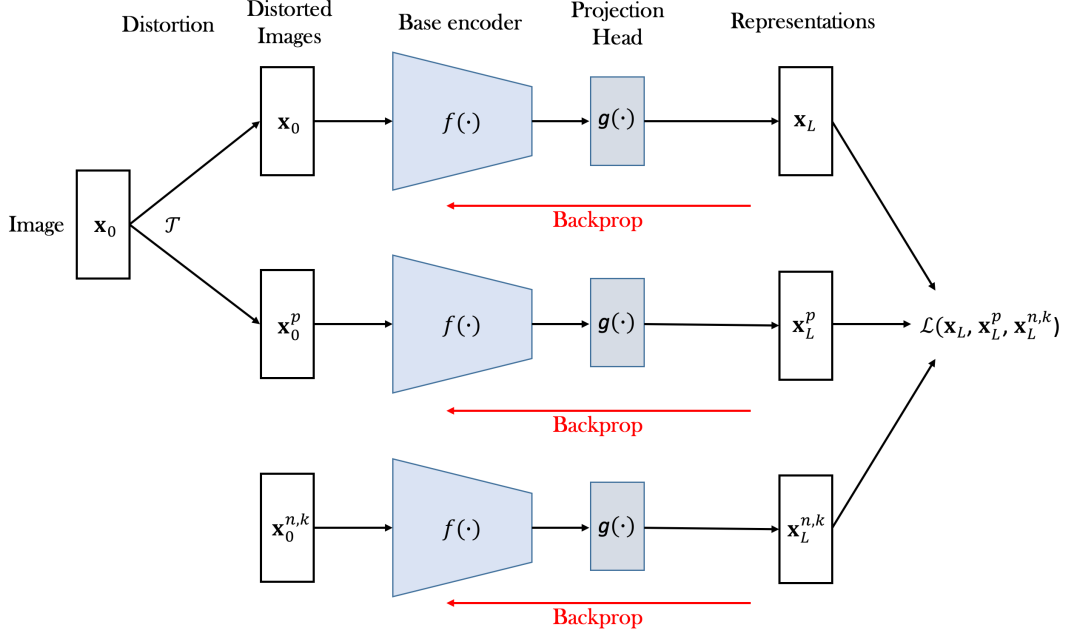


Figure 2: Graphical illustration of the contrastive learning framework.

and a projection head $g(\cdot)$ (usually an MLP that reduces the embedding size) that produce the final embeddings \mathbf{x}_L and \mathbf{x}_L^p (assuming in total L layers in the network), which we call a pair of positives. In contrastive learning methods such as [12] and [13], a set of other images, denoted as $\mathbf{x}_0^{n,k}$, $k = 1, \dots, K$, are also fed into the same $f(\cdot)$ and $g(\cdot)$ to produce the negative embeddings $\mathbf{x}_L^{n,k}$ to contrast with the positive. In SIMCLR, K is associated with the batch size; in MoCo, K is a free hyperparameter usually greater than the batch size. The networks are then trained to minimize the distance between \mathbf{x}_L and \mathbf{x}_L^p , i.e. to maximize the agreement between the two related views, and to maximize the distance between \mathbf{x}_L and $\mathbf{x}_L^{n,k}$'s in order to prevent collapsing. The training objective consists of these two components and we refer to it as the SIMCLR loss in this work:

$$\mathcal{L}_{\text{SIMCLR}} = -\log \frac{\exp(\text{sim}(\mathbf{x}_L, \mathbf{x}_L^p)/\tau)}{\exp(\text{sim}(\mathbf{x}_L, \mathbf{x}_L^p)/\tau) + \sum_{k=1}^K \exp(\text{sim}(\mathbf{x}_L, \mathbf{x}_L^{n,k})/\tau)} \quad (17)$$

where $\text{sim}(\mathbf{a}, \mathbf{b}) = \mathbf{a} \cdot \mathbf{b} / \|\mathbf{a}\|_2 \|\mathbf{b}\|_2$ and τ denotes a temperature hyperparameter. Notice that to make sure the similarity measurements are at the same scale across all data points, the embeddings \mathbf{x}_L , \mathbf{x}_L^p and $\mathbf{x}_L^{n,k}$ have been normalized to unit norm. This loss can be viewed as a multinomial logistic loss with predictor x_L and $K + 1$ classes, and the observed class corresponds to the positive x_L^p . Figure 2 gives an illustration of the training of the base encoder using contrastive learning.

Most SSL methods use linear evaluation to assess whether the pre-trained base encoders $f(\cdot)$ produce embeddings that are “good enough”. After training, the parameters in the base encoders (excluding the projection head) are locked, and images with class labels are passed into this fixed encoder to be projected into an embedding space. A linear classifier is then

trained based on the embeddings of these images that can report a classification accuracy. It has been shown by multiple studies, that embeddings from base encoders trained by BP are able to give classification performance comparable to encoders trained by supervised techniques on various datasets. In this work we train the base encoders using biologically plausible learning rules and compare their performance to those trained by BP. Before that, we first discuss the biological plausibility of SSL per se.

Biological Plausibility of SSL. SSL is a biologically more plausible training method than supervised learning not only because of its unsupervised nature, but also due to its property of perturbation invariance. As the network parameters are trained primarily to maximize the agreement between positive pairs created through a universal image transformation step, rather than class labels that are local to the training dataset, intuitively the network is robust enough to generalize to different datasets. This is similar to how humans learn: only a small portion of learning, especially at early stages of development, is through supervision, and humans can easily generalize what they learned on one dataset (e.g. one that consists of cats and dogs) to another one (e.g. one made up of lions and wolves). These two properties make SSL a promising model of learning in biological systems.

However, there remains an issue of the self-supervised loss functions described above: it is still unclear how exactly a biological neural circuit could propagate the error signals from these objectives to inform the update of the synaptic weights. The derivatives of the SIMCLR loss require complex computations consisting of a normalization step and a softmax step both involving ratios, as well as the inner product step. Here we provide a contrastive loss that is closely related to the losses proposed in [2] for supervised learning, which is simple enough to be computed by neural circuits.

In the topmost layer of a feedforward network the weight update is directly associated with the self-supervised loss. Formally, we write the forward computation occurring in the top layer as $\mathbf{x}_L = \mathbf{W}_L \mathbf{x}_{L-1}$. Notice that in the setting of SSL, the positive example of \mathbf{x}_0 , \mathbf{x}_0^p , and negatives $\mathbf{x}_0^{n,k}$ are passed through the same network and thus experience the same top-layer computation: $\mathbf{x}_L^p = \mathbf{W}_L \mathbf{x}_{L-1}^p$ and $\mathbf{x}_L^{n,k} = \mathbf{W}_L \mathbf{x}_{L-1}^{n,k}$. A self-supervised loss $\mathcal{L}(\mathbf{x}_L, \mathbf{x}_L^p, \mathbf{x}_L^{n,k})$ will then be calculated. During learning the update of \mathbf{W}_L is as follows:

$$\frac{\partial \mathcal{L}(\mathbf{x}_L, \mathbf{x}_L^p, \mathbf{x}_L^{n,k})}{\partial \mathbf{W}_L} = \frac{\partial \mathcal{L}(\mathbf{x}_L, \mathbf{x}_L^p, \mathbf{x}_L^{n,k})}{\partial \mathbf{x}_L} \mathbf{x}_{L-1} \quad (18)$$

If we denote the error signal $\frac{\partial \mathcal{L}(\mathbf{x}_L, \mathbf{x}_L^p, \mathbf{x}_L^{n,k})}{\partial x_{L,i}} = \delta_{L,i}$ and consider only single-unit computations, this is:

$$\frac{\partial \mathcal{L}(\mathbf{x}_L, \mathbf{x}_L^p, \mathbf{x}_L^{n,k})}{\partial W_{L,ij}} = \frac{\partial \mathcal{L}(\mathbf{x}_L, \mathbf{x}_L^p, \mathbf{x}_L^{n,k})}{\partial x_{L,i}} x_{L-1,j} = \delta_{L,i} x_{L-1,j} \quad (19)$$

For this top-layer learning rule to be Hebbian, we want the error signal $\delta_{L,i}$ to be local, including computations related only to neuron i . However, the SIMCLR contrastive loss (17) does not satisfy this condition. The error signal from this loss is:

$$\delta_{L,i} = \frac{\partial \mathcal{L}_{\text{SIMCLR}}}{\partial x_{L,i}} = \frac{\sum_{k=1}^K (x_{L,i}^{n,k} / \|\mathbf{x}_L^{n,k}\| - x_{L,i}^p / \|\mathbf{x}_L^p\|) \exp(\text{sim}(\mathbf{x}_L, \mathbf{x}_L^{n,k}) / \tau)}{\tau \|\mathbf{x}\| \left(\exp(\text{sim}(\mathbf{x}_L, \mathbf{x}_L^p) / \tau) + \sum_{k=1}^K \exp(\text{sim}(\mathbf{x}_L, \mathbf{x}_L^{n,k}) / \tau) \right)} \quad (20)$$

Several observations can be made from this error signal. First it is a weighted sum of $x_{L,i}^{n,k} / \|\mathbf{x}_L^{n,k}\| - x_{L,i}^p / \|\mathbf{x}_L^p\|$ over the K negatives, with weights being the similarity between the original embedding and the corresponding negative example, and second, to compute the error signal of the i th neuron, it is necessary to compute complex ratios and quantities related to the output of the other neurons in this layer, making the learning rule in equation (19) non-local. Furthermore all the computations are performed on normalized outputs. Although some evidence has been found for this type of computation in cortex, see [34], the instances are usually at lower levels of sensory input and involve local computations with neurons of similar types of responses. In our case we require normalization over a set of neurons with very diverse responses to very high level functions of the input, so a simpler learning rule avoiding such operations is preferable.

We propose an alternative contrastive loss inspired by the biologically plausible supervised loss in [2], which requires only local activities of the neurons in the top layer, and does not require normalization, thus lending itself to very simple network implementations. We call it the ‘‘contrastive hinge loss’’. For a single embedding \mathbf{x}_L and its positive and negative pairs, the loss is:

$$\mathcal{L}_{\text{hinge}} = [\|\mathbf{x}_L - \mathbf{x}_L^p\|_1 - m_1]_+ + \sum_{k=1}^K [m_2 - \|\mathbf{x}_L - \mathbf{x}_L^{n,k}\|_1]_+ \quad (21)$$

Only positives with a distance greater than a margin (m_1), and negatives with a distance smaller than a margin (m_2) will be selected, making sure that optimization only depends on ‘problematic’ examples. The error signal of this loss is:

$$\delta_{L,i} = \frac{\partial \mathcal{L}_{\text{hinge}}}{\partial x_{L,i}} = \mathbb{1}_{\|\mathbf{x}_L - \mathbf{x}_L^p\|_1 > m_1} \text{sgn}(x_{L,i} - x_{L,i}^p) - \sum_{k=1}^K \mathbb{1}_{\|\mathbf{x}_L - \mathbf{x}_L^{n,k}\|_1 < m_2} \text{sgn}(x_{L,i} - x_{L,i}^{n,k}) \quad (22)$$

During learning, this error signal will only depend on activities local to the i th neuron in the topmost layer. The only information needed from other neurons in the output is in filtering out the ‘‘easy’’ negatives involving L1 distances between activities. These can be quite easily implemented in a network with rectified units and a combination of excitatory and inhibitory neurons. Moreover no normalization is needed.

4 Experiments

4.1 Linear evaluation on CIFAR10

We first verify our hypothesis, that networks trained by our biologically learning rules produce embeddings with representational powers as strong as that by BP. We use the standard

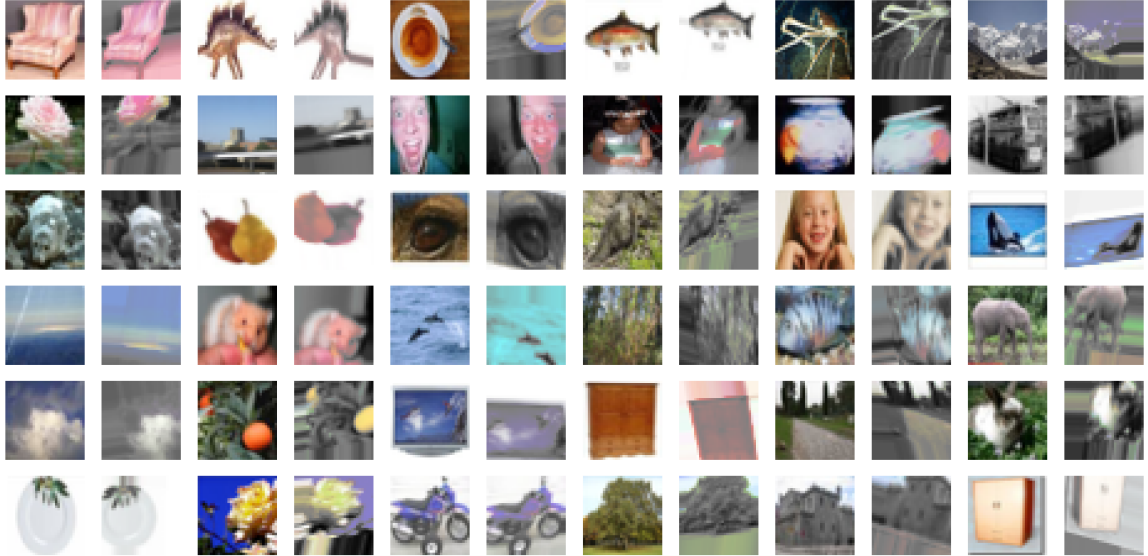


Figure 3: Examples of CIFAR100 images (left) and their transformed versions (right).

linear evaluation scheme with CIFAR100 and CIFAR10 [35] for this set of experiments. The network architecture we use is as follows:

```

Conv 32 3x3 1; Hardtanh;
Conv 32 3x3 1; Maxpool 2;
Conv 64 3x3 1; Hardtanh;
Conv 64 3x3 1; Maxpool 2;
Conv 512 3x3 1; Maxpool 2;
Dense 64

```

where `Conv 32 3x3` stands for a convolutional layer with filter size 3 and channel number 32, and `Maxpool 2` stands for a max pooling layer with filter size 2 and stride size 2, which reduces the image size by a factor of 2. We use CIFAR100 to train this base encoder. At training time, each instance of CIFAR100 will be distorted randomly, and some examples of the original and distorted images can be seen in Figure 3. The original image and the distorted version will form the positive pair, and all other images within the mini-batch will form the negatives. All these images are passed into the base encoder and the encoder produces 64-dimensional embeddings of these images, which are used to calculate the self-supervised loss. The parameters of the encoder are updated to minimize this loss.

After the base encoders are trained, we fix their parameters and remove the last dense layer, called the head. We use the fixed layers to produce embeddings (the output of the last convolutional layer) as inputs to a linear classifier, trained on 45000 CIFAR10 examples and

Loss	Learning	Update	Classifier acc.
Contr. Hinge	E2E	BP	71.44%
		DTP	71.29%
		RF	61.70%
	GLL	BP/URF	72.76%
		RF	67.83%
	RLL	BP/URF	71.35%
		RF	65.94%
SIMCLR	E2E	BP	72.44%
Rnd. encoder		61.23%	

Table 1: Classification accuracy on CIFAR10 using the pre-trained networks with SSL.

tested on 10000 CIFAR10 examples. The training of the linear classifier is supervised, and we use the classification accuracy as a measure of the representational power of the embeddings. We choose to use different datasets for training the encoders and classifiers because this is a more realistic learning scenario for biological systems: rather than learning from tasks on an ad hoc basis, the brain learns from more generic tasks and data, and applies the learned synaptic weights to other tasks (e.g. classification).

For all experiments, we train the base encoder networks for 400 epochs using the Adam optimizer, with a learning rate 0.0001. Particularly, in DTP we use a fixed learning rate 0.001 for the layer-wise autoencoders. For the contrastive losses we train the base encoders with a batch size of 500. The linear classifiers are trained using the Adam optimizer with a learning rate 0.001 for 400 epochs. For hyperparameters for the contrastive losses, we use $\tau = 0.1$ for the SIMCLR loss and $m_1 = 1, m_2 = 3$ for the contrastive hinge loss, based on the initial distance distributions between positives and negatives in an arbitrary batch (Figure 4). Table 1 shows our experimental results. It can be seen that the proposed, biologically more plausible contrastive hinge loss achieves similar performance to the SIMCLR loss baseline. Overall, the biologically plausible learning rules achieve comparable linear evaluation performance to end-to-end BP. Layer-wise learning performs similarly to end-to-end learning with BP. There is some loss of accuracy with RF layer-wise learning but it still performs much better than end-to-end RF. In fact, the performance of end-to-end RF is close to that of a random encoder, which further demonstrates the failure of RF in deep networks.

Furthermore, when a batch size consisting of hundreds of samples is used, there are hundreds of negative pairs in the self-supervised loss computation, for each positive pair. It would appear more natural that each positive is contrasted against a small number of negative pairs. We experimented with computing the contrastive hinge loss, with only 5 randomly chosen negative images from the full batch and obtained identical results.

Notably, while earlier works with supervised learning [15, 10] have shown a relatively large difference between BP and DTP, in SSL we observe close performance between these two learning rules. Figure 6 shows how the values of the contrastive hinge loss evolves using different training methods.

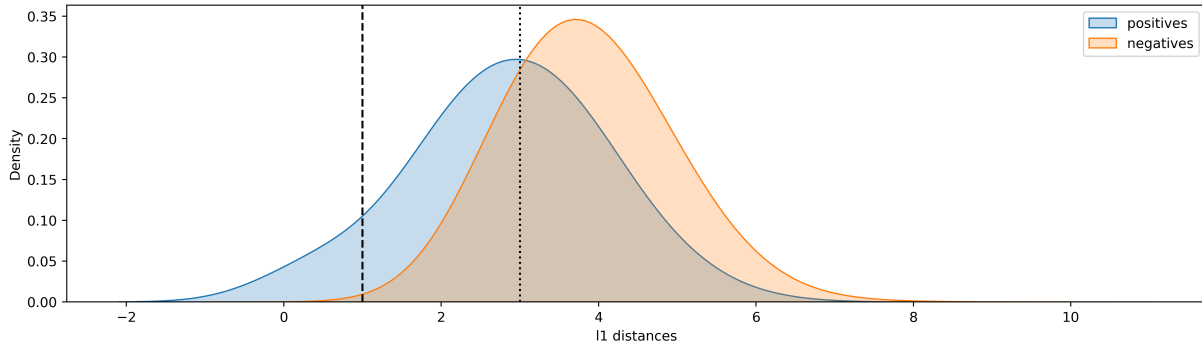


Figure 4: The initial distance distributions between positives and negatives in an arbitrary batch, fitted using kernel density estimation. Dashed line indicates the margin for positives and dotted line indicates the margin for negatives.

Pooling vs Strided Convolution in DTP. We compare the linear evaluation performance of the encoder networks using two different down-sampling techniques, namely the max pooling layers and the strided convolutional layers, when the networks are trained by DTP. When using max pooling layers, the linear evaluation performance is 71.29% for DTP respectively (Table 1). However, this number quickly drops to 39.42% with strided convolutional layers. Even for straightforward supervised classification training on CIFAR10, with the same architecture, there is a significant advantage using max pooling compared to strided convolution in conjunction with DTP, 71% vs. 58%. This result demonstrates that pooling layers are not only compatible with DTP, but are also better down-sampling techniques in certain architectures.

End-to-End and Layer-wise Learning. Figure 5 compares the linear evaluation performance of end-to-end and layer-wise learning with BP/URF and RF, respectively. We can see that the layer-wise learning achieves similar, if not better, accuracy compared to the traditional end-to-end learning with BP updates. It is known that RF updates do not work well with deep networks when trained with end-to-end learning. Layer-wise learning with RF works around the problem by only updating one layer at a time and improves the performance by a large margin compared to end-to-end training with RF.

We examine the loss of self-supervised training in Figure 6 to further understand the behavior and convergence of the two layer-wise learning method. The networks are trained sequentially with GLL, and we calculate the average training loss after each epoch, while a layer is trained. The training loss has a significant jump when a new layer is added to the top of the network, and then rapidly decreases to values lower than the previous layer and converges. For RLL, different layers are selected for each batch of data, and the training loss is an average among all batches, and hence all layers, in an epoch. The average training loss slightly oscillates and converges. Note that the values of the RLL loss cannot be directly compared to the loss of GLL since the training loss for RLL is an average across all layers.

The results show that layer-wise learning could be a more biologically plausible alternative to end-to-end learning. In addition, the effectiveness of RLL further indicates that it is not

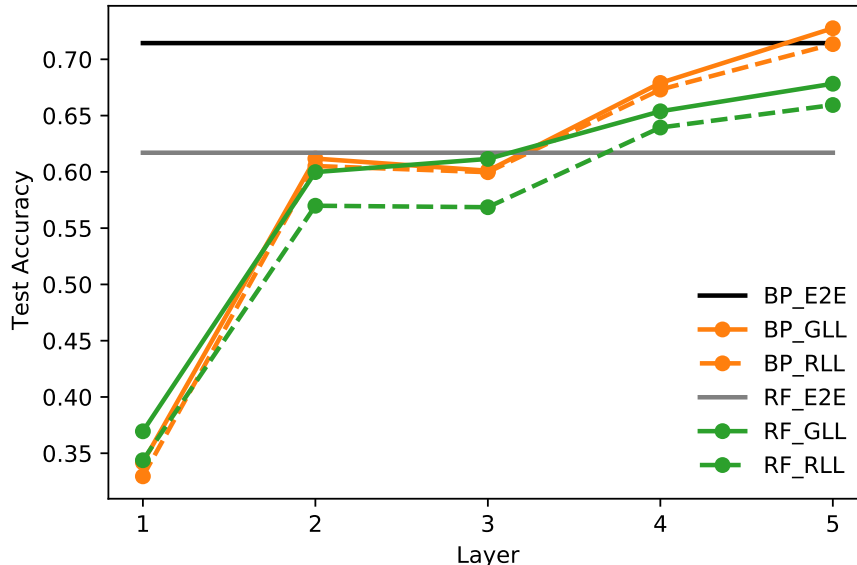


Figure 5: Test accuracy of the network trained with Hinge loss and End-to-End (E2E) learning, Greedy Layer-wise Learning (GLL) and Randomized Layer-wise Learning (RLL) and updating with Back-propagation (BP) and Random Feedback (RF)

necessary to train the layers sequentially. Randomly selecting a layer to update and training all layers simultaneously gives competitive results compared to sequential layer-wise training.

Training Data for the Encoder Networks. So far, we have only discussed the circumstance where we train the base encoders on CIFAR100, and test the “goodness” of the embeddings produced by the encoders given CIFAR10 in test time. We choose to test the embeddings on a different dataset, to mimic the brain’s ability to apply generically learned synapses to specific tasks. Intuitively, one may claim that training and testing on the same dataset should outperform our approach, as the encoders would inevitably learn features that are local to the training data. Surprisingly, our result shows that the linear classifier performs equally well on CIFAR10 when the base encoders are trained on CIFAR100 and CIFAR10, and far better than the random base encoder. This result suggests that the SSL framework learns the generic, global features **only**, and should thus be more robust to perturbation, which makes it a biologically more plausible framework than supervised learning. Our next set of experiments strengthens this argument.

4.2 Transfer to noise-perturbed data

For further explorations of the perturbation invariant property of SSL, we use two other sets of data, namely the 28×28 gray-scale digits [36] and letters [37]. We first train the base encoders on the letters data, and then we use the trained encoders to produce embeddings of the digits data (MNIST) and train a linear classifier on these embeddings. We then test the

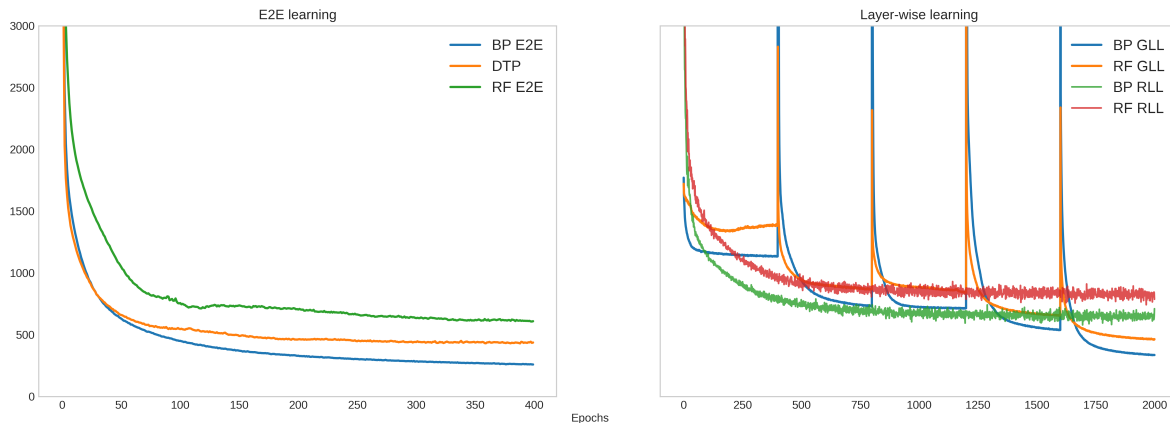


Figure 6: Evolution of the contrastive hinge loss during training (excessively large values are cut off to maintain visibility).

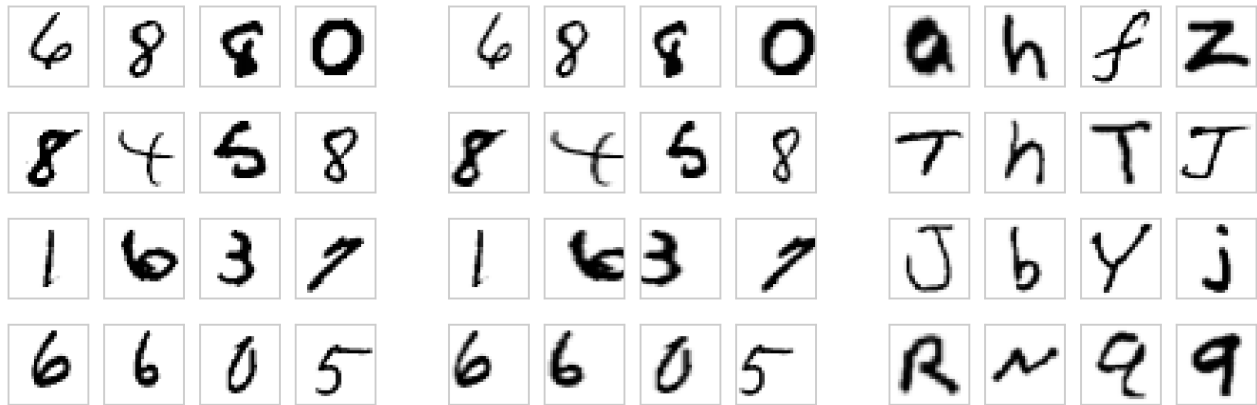


Figure 7: Examples of MNIST digits (left), transformed MNIST digits (middle) and letters (right) data.

classifiers on their ability to classify a set of affine-transformed digits (transformed MNIST) and report its accuracy. Some examples of these three datasets are shown in Figure 7. This experiment design aims to verify the robustness of the SSL framework, by comparing its performance with a fully supervised CNN trained by MNIST and tested on transformed MNIST. For this set of experiments, we use a CNN with the following architecture:

```
Conv 32 3x3 1; Maxpool 2; Tanh;
Conv 64 3x3 1; Maxpool 2; Tanh;
Conv 128 3x3 1; Maxpool 2; Tanh;
Dense 64
```

We note that for the relatively easy task of classifying MNIST digits, all the unsupervised training methods perform above 98%, even using end to end feedback alignment. After all a

Loss	Learning	Update	Classifier acc. on transformed digits
Contr. Hinge	E2E	BP	80.20%
		DTP	81.37%
		RF	75.89%
	GLL	BP	81.31%
		RF	80.86%
	RLL	BP	80.31%
		RF	78.52%
SIMCLR	E2E	BP	81.96%
Supervised			75.6%
Rnd. encoder			62.66%

Table 2: Test accuracy on transformed MNIST using the pre-trained networks with SSL on letters. Classifiers trained on original MNIST.

random network with this structure, where we only train the linear classification layer, also yields above 98% accuracy. Thus the interesting question is how well does the unsupervised network generalize to the transformed digits.

We train the base encoder networks for 400 epochs using the Adam optimizer, with a learning rate chosen between $[0.0001, 0.001]$. In DTP, we again use a fixed learning rate 0.001 for the layer-wise auto-encoders. We train the base encoders with a batch size 1000, and the linear classifier is trained for 200 epochs using Adam optimizer with a learning rate of 0.001. We use $m_1 = 1$, $m_2 = 1.5$ for the contrastive hinge losses. The results with contrastive methods are shown in Table 2.

We found that all classification results on the the transformed data are substantially better than those obtained by training the linear classifier using a random base encoder. In addition, classification results are better than those by training a supervised network with MNIST digits and testing it on transformed MNIST digits. These results further illustrate the perturbation robustness property of our proposed framework and suggests that SSL produces informative features for downstream classification tasks.

5 Discussion

In this work we have shown that it is possible to construct a biologically plausible deep learning framework using self-supervised learning (SSL) combined with layer-wise learning or difference target propagation (DTP). We have also introduced a more biologically plausible contrastive loss. An embedding is learned through the self-supervised contrastive loss using one collection of images. The evaluation of the embedding is done by training a linear classifier, taking as input the trained embedding, but using a separate collection of labeled digits from different categories.

For DTP we have found that pooling layers are compatible with DTP and performs better in our network architectures than strided convolutional layers with self-supervised objectives.

Layer-wise learning requires physical connections between each layer and the error computing layer. This is consistent with the fact that direct connections do exist between various retinotopic layers and higher cortical areas [38]. And the fact that randomized layer-wise training is effective means that there is no need to sequence the learning of the different layers.

Using these alternative learning methods, we have produced comparable embeddings to the backprop-trained ones for linear evaluation. We have shown that the perturbations inherent in the self-supervised learning yield embeddings that are more robust to variation than direct classifier training. Furthermore we have shown that there is no need for large numbers of negative examples for each positive pair in order to obtain the same results. A future direction of research would involve actually training on continuous videos of moving objects, with small buffers for the negative images.

Considering the approach of using ANNs as models of cortical areas in general, although [3] have shown that CNNs are similar to the ventral visual stream in a lot of ways, including the end-to-end behavior and the unit-level activities, many aspects of CNNs are still far from biologically realistic. For example, units in CNNs are continuously valued, while real neurons are discrete, emitting binary spikes. Even if we use CNNs to simply model the firing rates of neurons, negative unit values are still a problem. Another source of implausibility is that CNNs involve only feedforward connections, while biological neurons in the cortex are also recurrently connected, with different connectivity patterns between different cell types and areas. Moreover, the weight sharing property of convolutional layers lacks neurobiological support, and using locally connected layers [15, 2] may be a more biologically plausible approach. To further develop our proposed framework, these aspects are definitely to be considered.

References

- [1] Timothy P. Lillicrap, Daniel Cownden, Douglas B. Tweed, and Colin J. Akerman. Random synaptic feedback weights support error backpropagation for deep learning. *Nature Communications*, 7:13276 EP –, 11 2016.
- [2] Yali Amit. Deep learning with asymmetric connections and hebbian updates. *Frontiers in computational neuroscience*, 13:18, 2019.
- [3] Daniel LK Yamins and James J DiCarlo. Using goal-driven deep learning models to understand sensory cortex. *Nature neuroscience*, 19(3):356–365, 2016.
- [4] Lane T McIntosh, Niru Maheswaranathan, Aran Nayebi, Surya Ganguli, and Stephen A Baccus. Deep learning models of the retinal response to natural scenes. *Advances in neural information processing systems*, 29:1369, 2016.
- [5] Nicolas Y Masse, Guangyu R Yang, H Francis Song, Xiao-Jing Wang, and David J Freedman. Circuit mechanisms for the maintenance and manipulation of information in working memory. *Nature neuroscience*, 22(7):1159–1167, 2019.
- [6] H Francis Song, Guangyu R Yang, and Xiao-Jing Wang. Training excitatory-inhibitory recurrent neural networks for cognitive tasks: a simple and flexible framework. *PLoS computational biology*, 12(2):e1004792, 2016.
- [7] David E Rumelhart, Geoffrey E Hinton, and Ronald J Williams. Learning representations by back-propagating errors. *nature*, 323(6088):533–536, 1986.
- [8] Timothy P Lillicrap, Adam Santoro, Luke Marris, Colin J Akerman, and Geoffrey Hinton. Backpropagation and the brain. *Nature Reviews Neuroscience*, 21(6):335–346, 2020.
- [9] David Zipser and David E Rumelhart. The neurobiological significance of the new learning models. In *Computational neuroscience*, pages 192–200. 1993.
- [10] Dong-Hyun Lee, Saizheng Zhang, Asja Fischer, and Yoshua Bengio. Difference target propagation. In *Joint european conference on machine learning and knowledge discovery in databases*, pages 498–515. Springer, 2015.
- [11] Mohamed Akrouf, Collin Wilson, Peter C Humphreys, Timothy Lillicrap, and Douglas Tweed. Deep learning without weight transport. *arXiv preprint arXiv:1904.05391*, 2019.
- [12] Ting Chen, Simon Kornblith, Mohammad Norouzi, and Geoffrey Hinton. A simple framework for contrastive learning of visual representations. In *International conference on machine learning*, pages 1597–1607. PMLR, 2020.
- [13] Kaiming He, Haoqi Fan, Yuxin Wu, Saining Xie, and Ross Girshick. Momentum contrast for unsupervised visual representation learning. In *Proceedings of the IEEE/CVF Conference on Computer Vision and Pattern Recognition*, pages 9729–9738, 2020.

- [14] S. Becker and Geoffrey E. Hinton. Self-organizing neural network that discovers surfaces in random-dot stereograms. *Nature*, 355:161–163, 1992.
- [15] Sergey Bartunov, Adam Santoro, Blake A Richards, Luke Marris, Geoffrey E Hinton, and Timothy Lillicrap. Assessing the scalability of biologically-motivated deep learning algorithms and architectures. *arXiv preprint arXiv:1807.04587*, 2018.
- [16] Geoffrey E Hinton, Simon Osindero, and Yee-Whye Teh. A fast learning algorithm for deep belief nets. *Neural computation*, 18(7):1527–1554, 2006.
- [17] Yoshua Bengio, Pascal Lamblin, Dan Popovici, and Hugo Larochelle. Greedy layer-wise training of deep networks. In *Advances in neural information processing systems*, pages 153–160, 2007.
- [18] Furong Huang, Jordan Ash, John Langford, and Robert Schapire. Learning deep resnet blocks sequentially using boosting theory. pages 2058–2067, 2018.
- [19] Eugene Belilovsky, Michael Eickenberg, and Edouard Oyallon. Greedy Layerwise Learning Can Scale to ImageNet. *arXiv:1812.11446 [cs, stat]*, April 2019.
- [20] Max Jaderberg, Wojciech Marian Czarnecki, Simon Osindero, Oriol Vinyals, Alex Graves, David Silver, and Koray Kavukcuoglu. Decoupled Neural Interfaces using Synthetic Gradients. *arXiv:1608.05343 [cs]*, July 2017.
- [21] Arild Nøkland and Lars Hiller Eidnes. Training Neural Networks with Local Error Signals. *arXiv:1901.06656 [cs, stat]*, May 2019.
- [22] Xinlei Chen and Kaiming He. Exploring simple siamese representation learning. *arXiv preprint arXiv:2011.10566*, 2020.
- [23] Qianli Liao, Joel Leibo, and Tomaso Poggio. How important is weight symmetry in backpropagation? In *Proceedings of the AAAI Conference on Artificial Intelligence*, volume 30, 2016.
- [24] Rajesh PN Rao and Dana H Ballard. Predictive coding in the visual cortex: a functional interpretation of some extra-classical receptive-field effects. *Nature neuroscience*, 2(1):79–87, 1999.
- [25] Michael W Spratling. A hierarchical predictive coding model of object recognition in natural images. *Cognitive computation*, 9(2):151–167, 2017.
- [26] James CR Whittington and Rafal Bogacz. Theories of error back-propagation in the brain. *Trends in cognitive sciences*, 23(3):235–250, 2019.
- [27] James CR Whittington and Rafal Bogacz. An approximation of the error backpropagation algorithm in a predictive coding network with local hebbian synaptic plasticity. *Neural computation*, 29(5):1229–1262, 2017.

- [28] Aaron van den Oord, Yazhe Li, and Oriol Vinyals. Representation learning with contrastive predictive coding. *arXiv preprint arXiv:1807.03748*, 2018.
- [29] Jean-Bastien Grill, Florian Strub, Florent Altché, Corentin Tallec, Pierre H Richemond, Elena Buchatskaya, Carl Doersch, Bernardo Avila Pires, Zhaohan Daniel Guo, Mohammad Gheshlaghi Azar, et al. Bootstrap your own latent: A new approach to self-supervised learning. *arXiv preprint arXiv:2006.07733*, 2020.
- [30] Jure Zbontar, Li Jing, Ishan Misra, Yann LeCun, and Stéphane Deny. Barlow twins: Self-supervised learning via redundancy reduction. *arXiv preprint arXiv:2103.03230*, 2021.
- [31] Horace B Barlow et al. Possible principles underlying the transformation of sensory messages. *Sensory communication*, 1(01), 1961.
- [32] Chengxu Zhuang, Siming Yan, Aran Nayebi, Martin Schrimpf, Michael C Frank, James J DiCarlo, and Daniel LK Yamins. Unsupervised neural network models of the ventral visual stream. *Proceedings of the National Academy of Sciences*, 118(3), 2021.
- [33] Martin Schrimpf, Jonas Kubilius, Ha Hong, Najib J Majaj, Rishi Rajalingham, Elias B Issa, Kohitij Kar, Pouya Bashivan, Jonathan Prescott-Roy, Kailyn Schmidt, et al. Brain-score: Which artificial neural network for object recognition is most brain-like? *BioRxiv*, page 407007, 2018.
- [34] Matteo Carandini and David J Heeger. Normalization as a canonical neural computation. *Nature Reviews Neuroscience*, 13(1):51–62, 2012.
- [35] Alex Krizhevsky, Geoffrey Hinton, et al. Learning multiple layers of features from tiny images. 2009.
- [36] Yann LeCun and Corinna Cortes. MNIST handwritten digit database. 2010.
- [37] Gregory Cohen, Saeed Afshar, Jonathan Tapson, and Andre Van Schaik. Emnist: Extending mnist to handwritten letters. In *2017 International Joint Conference on Neural Networks (IJCNN)*, pages 2921–2926. IEEE, 2017.
- [38] David C. Van Essen, Chad J. Donahue, Timothy S. Coalson, Henry Kennedy, Takuya Hayashi, and Matthew F. Glasser. Cerebral cortical folding, parcellation, and connectivity in humans, nonhuman primates, and mice. *Proceedings of the National Academy of Sciences*, 116(52):26173–26180, 2019.